Science Advances

AAAS

advances.sciencemag.org/cgi/content/full/2/10/e1601086/DC1

Supplementary Materials for

Quasi-particle interference of heavy fermions in resonant x-ray scattering

András Gyenis, Eduardo H. da Silva Neto, Ronny Sutarto, Enrico Schierle, Feizhou He, Eugen Weschke, Mariam Kavai, Ryan E. Baumbach, Joe D. Thompson, Eric D. Bauer, Zachary Fisk, Andrea Damascelli, Ali Yazdani, Pegor Aynajian

Published 14 October 2016, *Sci. Adv.* **2**, e1601086 (2016)
DOI: 10.1126/sciadv.1601086

This PDF file includes:

STM measurements and data analysis

The reported STM conductance maps were acquired on a 475 Å x 475 Å (x = 0.15) and on a 400 Å x 400 Å (x = 0.0075) large square area (fig. S1, A and B), by applying a lock-in oscillation of 0.5 meV at a parking bias of −100 meV and setpoint currents of 1.6 nA (x = 0.15) and 1 nA (x = 0.0075). The features were reproduced at different tunneling junction impedances. The bright spots on the topographic images correspond to the Cd dopants. The spatially averaged *dI/dV* spectra on both samples show the double-peak feature (fig. S1C) demonstrating the heavy band formation at T = 10 K independently of the underlying ground state in $CeCo(In_{1-x}Cd_x)_5$.

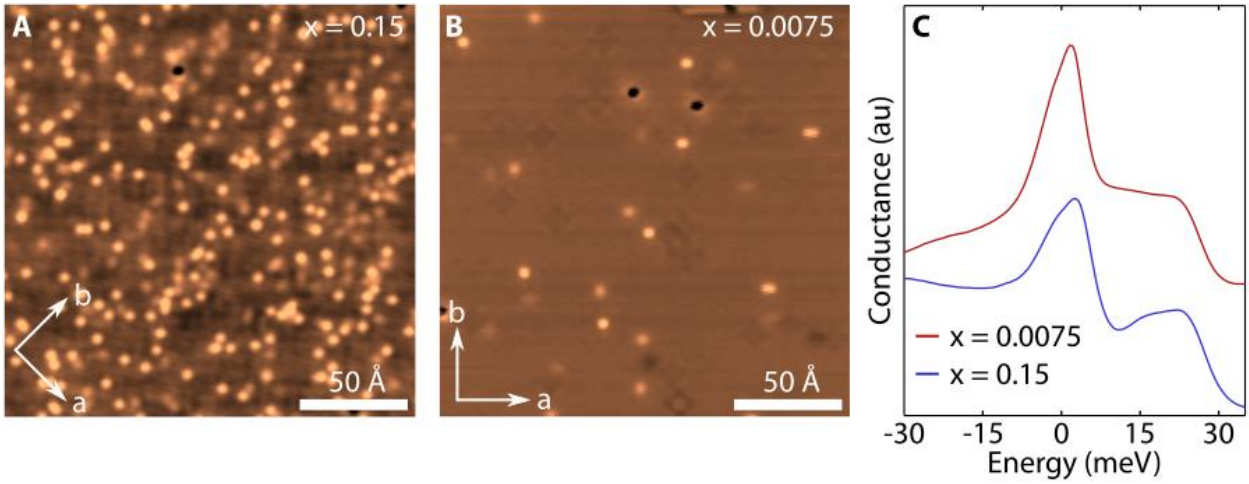

fig. S1. STM measurements on $CeCo(In_{1-x}Cd_x)_5$. Topographic image of (**A**) x = 0.15 and (**B**) x = 0.0075 Cd-doped samples. Bright (dark) corresponds to high (low) topography. (**C**) Spatially averaged tunneling conductance on surface B on the two samples.

In the real space conductance maps, the conductance values on the Cd impurities observable on the topographic image were replaced by the average conductance value at the given energy to suppress the high / low tunneling value into a bound state of the Cd dopant, which is independent from the quasiparticle interference. The real space maps were normalized by their mean prior to taking the Fourier transformation, which allows us to directly compare the modulation strength at

different energies. Finally, the Fourier transform of the maps were symmetrized based on the symmetry of the underlying lattice (mirror symmetry along the *a* and *b* axis and also 90 degrees rotation about the *c* axis) to eliminate the effects of the random shape of the STM tip (fig. S2). We note that the reported features are apparent without any of the manipulation and the described procedure serves only the purpose of enhancing the signal to noise ratio.

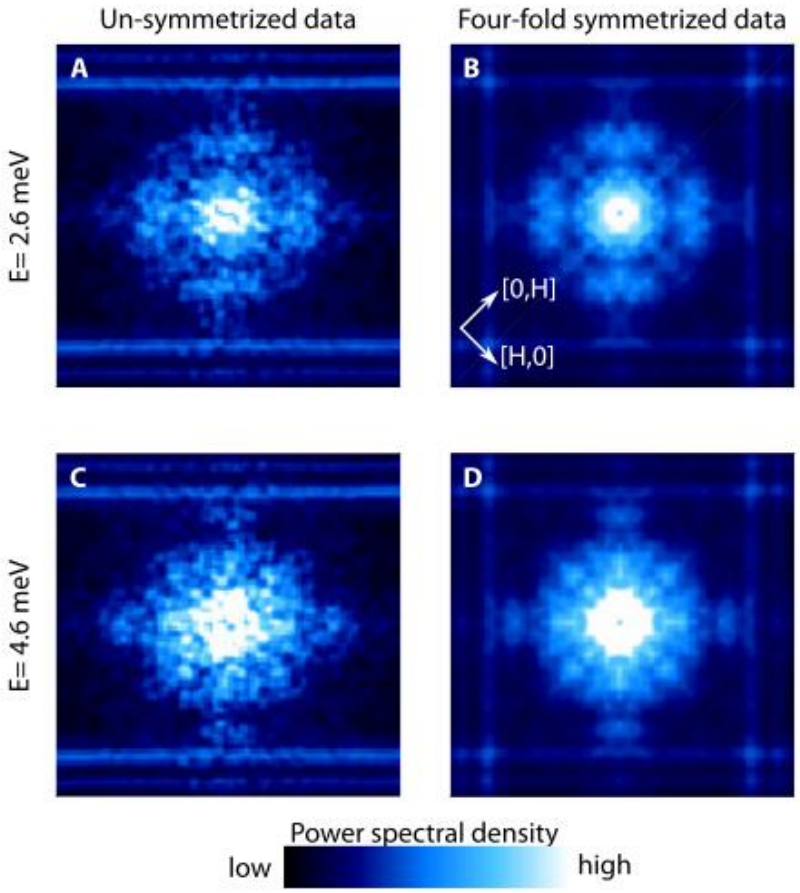

fig. S2. Symmetrization of the conductance map. (**A**) and (**C**) Fourier transform of the real space conductance maps shown in Fig. 1, C and D before symmetrization. (**B**) and (**D**) Four-fold symmetrized conductance map on a single colorscale.

RXS comparison on Cd-doped sample

As we discussed it in the main text, we observed the same RXS peak enhancement in the cases of the pure and the 10% Cd-doped sample (Fig. 3C). Here, we show additional temperature dependence of the RXS peaks, which exhibit remarkably similar behavior. As fig. S3 demonstrates, the RXS peak is absent above the hybridization temperature T^* in both samples.

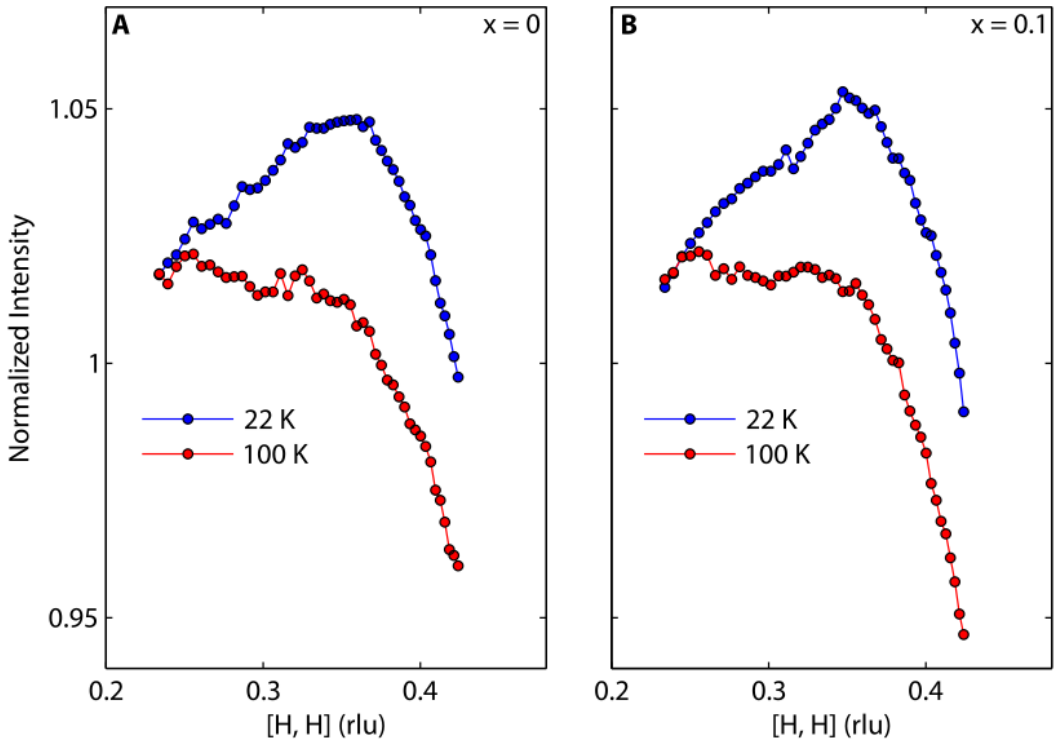

fig. S3. Comparison of the RXS cross section on $CeCo(In_{1-x}Cd_x)_5$. Temperature dependence of the RXS signal on (**A**) pure and (**B**) x = 0.1 Cd-doped samples at T = 22 K and 100 K.

***L* dependence of the RXS enhancement**

Since the momentum scans are not restricted to a single L value, our RXS measurement probes the scattering signal on a cut [$H(\theta_{sample}, \theta_{det})$, $H(\theta_{sample}, \theta_{det})$, $L(\theta_{sample}, \theta_{det})$] through reciprocal space determined by the sample (θ_{sample}) and detector angles (θ_{det}). Therefore, it is more complicated than the surface investigated by STM. Figure S4 displays the L dependence of the scattering peak on the top axis of the plot, which shows that the broad peak exists on a wide

range of L. More importantly, since $CeCoIn_5$ has a three-dimensional band-structure, the two techniques might measure different k_z components of the band structure and a truly direct comparison of the two results is not possible, as it is discussed in details in the main text.

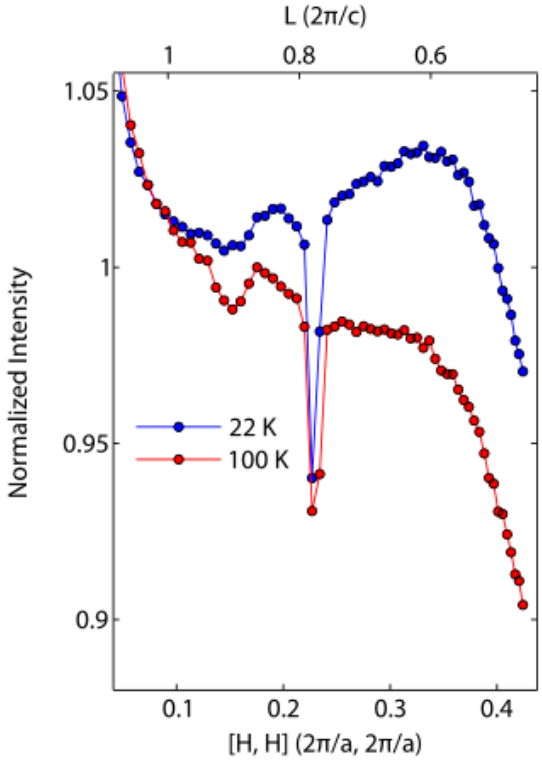

fig. S4. *L* dependence of the RXS measurement. The observed RXS peaks at T = 22 K and 100 K with their L dependence indicated on the top axis.

Anomalous drop in the RXS signal

As Fig. 3 shows, the measured RXS scattering amplitude exhibits a sharp drop near H = 0.22 rlu along the [H, H] direction. Although the origin of this feature is unknown, its relative sharpness, temperature- and doping-independence suggest that it is related to some kind of destructive interference in the scattering process.